MABS
2023, VOL. 15, NO. 1, e2149057 (15 pages)
https://doi.org/10.1080/19420862.2022.2149057

Taylor & Francis
Taylor & Francis Group

REPORT

OPEN ACCESS Check for updates

A glyco-engineering approach for site-specific conjugation to Fab glycans

Maria L. Jaramillo[a], Traian Sulea[a], Yves Durocher[a], Mauro Acchione[a], Melissa J. Schur[b], Anna Robotham[b], John F. Kelly[b], Marie-France Goneau[b], Alma Robert[a], Yuneivy Cepero-Donates[a], and Michel Gilbert[b]

[a]Human Health Therapeutics Research Centre, National Research Council Canada, 6100 Royalmount Avenue, H4P 2R2, Montreal, Qc, Canada; [b]Human Health Therapeutics Research Centre, National Research Council Canada, 100 Sussex Drive, K1A 0R6, Ottawa, ON, Canada

ABSTRACT

Effective processes for synthesizing antibody-drug conjugates (ADCs) require: 1) site-specific incorporation of the payload to avoid interference with binding to the target epitope, 2) optimal drug/antibody ratio to achieve sufficient potency while avoiding aggregation or solubility problems, and 3) a homogeneous product to facilitate approval by regulatory agencies. In conventional ADCs, the drug molecules are chemically attached randomly to antibody surface residues (typically Lys or Cys), which can interfere with epitope binding and targeting, and lead to overall product heterogeneity, long-term colloidal instability and unfavorable pharmacokinetics. Here, we present a more controlled process for generating ADCs where drug is specifically conjugated to only Fab *N*-linked glycans in a narrow ratio range through functionalized sialic acids. Using a bacterial sialyltransferase, we incorporated *N*-azidoacetylneuraminic acid (Neu5NAz) into the Fab glycan of cetuximab. Since only about 20% of human IgG1 have a Fab glycan, we extended the application of this approach by using molecular modeling to introduce *N*-glycosylation sites in the Fab constant region of other therapeutic monoclonal antibodies. We used trastuzumab as a model for the incorporation of Neu5NAz in the novel Fab glycans that we designed. ADCs were generated by clicking the incorporated Neu5NAz with monomethyl auristatin E (MMAE) attached to a self-immolative linker terminated with dibenzocyclooctyne (DBCO). Through this process, we obtained cetuximab-MMAE and trastuzumab-MMAE with drug/antibody ratios in the range of 1.3 to 2.5. We confirmed that these ADCs still bind their targets efficiently and are as potent in cytotoxicity assays as control ADCs obtained by standard conjugation protocols. The site-directed conjugation to Fab glycans has the additional benefit of avoiding potential interference with effector functions that depend on Fc glycan structure.

ARTICLE HISTORY
Received 23 July 2022
Revised 30 October 2022
Accepted 15 November 2022

KEYWORDS
Actinobacillus; antibody; cetuximab; drug conjugate; Fab glycan; sialyltransferase; trastuzumab

Introduction

Antibody conjugates are useful for delivering payloads, including but not limited to therapeutic and/or diagnostic agents, to specific targets. The manufacturing of antibody conjugates using conventional chemistry approaches non-selectively links cargo to antibodies by electrophilic modification of surface lysine or cysteine residues using *N*-hydroxysuccinimide (NHS) ester or maleimide-activated drugs, respectively.[1] These conjugation methods yield heterogeneous mixtures of products whose distributions differ in the sites and stoichiometry of modification. Nonspecific incorporation of the cargo on the antibody can result in a conjugate that has reduced targeting as compared to antibody alone if the incorporation happens in a region of the antibody involved with binding of the epitope, or reduced Fc effector functions if the incorporation is in a region involved with Fc effector functions. In addition, production of a heterogenous product may lead to difficulties in obtaining an optimal cargo-to-antibody ratio. Finally, the resulting heterogeneous mixture can substantially affect the manufacturing process, the pharmacokinetic properties of the antibody-drug conjugates (ADCs) and the efficacy in vivo.[2] Therefore, there is a high interest in the development of site-specific conjugation methodologies that avoid these problems.

More homogeneous ADCs have been obtained by genetic engineering of antibodies to incorporate additional cysteines,[3] unnatural amino acids[4–6] or tags for transamination reactions.[7] Non-genetic methods for generating antibody conjugates (i.e., that rely on the native mAb sequence) have been developed by modifying naturally occurring glycan residues for the purpose of attaching payloads. IgGs are modified by a structurally heterogeneous *N*-linked glycan at the conserved Asn297 residue, located in the constant CH2 domain of the Fc region. Since this glycan modification lies far away from the variable region of IgGs, it is unlikely to affect antigen-binding properties and is an attractive site for chemical or enzymatic modifications of monoclonal antibodies (mAbs). The glycan chain itself can be considered as an hydrophilic "linker extension" that should facilitate the conjugation of payloads that can be bulky and/or hydrophobic. Glycan-based antibody conjugation is achieved by introducing a chemically reactive moiety into the *N*-glycan, followed by conjugation to a payload carrying a matching chemically reactive group.

CONTACT Michel Gilbert michel.gilbert@nrc-cnrc.gc.ca Human Health Therapeutics Research Centre, National Research Council Canada, 100 Sussex Drive, K1A 0R6 Ottawa, ON, Canada.

Supplemental data for this article can be accessed online at https://doi.org/10.1080/19420862.2022.2149057

© 2022 Crown Copyright. Published with license by Taylor & Francis Group, LLC.
This is an Open Access article distributed under the terms of the Creative Commons Attribution-NonCommercial License (http://creativecommons.org/licenses/by-nc/4.0/), which permits unrestricted non-commercial use, distribution, and reproduction in any medium, provided the original work is properly cited.

Many strategies have been developed to introduce a chemically reactive group into the *N*-linked glycans of mAbs.[8] Metabolic engineering has been used to introduce sugar analogs containing biorthogonal reactive groups. Okeley et al. incorporated a thiolated fucose analog into the *N*-glycans of two mAbs and used maleimide chemistry to produce ADCs.[9] Alternatively, *N*-glycans can be oxidized using periodate to generate an aldehyde group at the glycan terminus that can be reacted with aminooxy-, hydrazine-, or hydrazide-functionalized payloads.[10,11] However, although site-specificity is achieved, undesirable oxidation of sensitive residues can potentially compromise the integrity and efficacy of mAbs.

More recent approaches involve enzymatic remodeling of the *N*-glycans in order to introduce a bioorthogonal reactive group under mild conditions. Wild-type (WT) or mutant glycosyltransferases can be used to add modified sugar residues to the termini of existing *N*-glycan "branches". When terminal GlcNAc residues are available, it is possible to add functionalized galactose or *N*-acetylgalactosamine residues using a mutant form (Y289L) of the β-1,4-galactosyltransferase I (B4GalT1) and subsequently conjugate a cytotoxic payload.[12–14] The ST6 β-galactoside α-2,6-sialyltransferase 1 (ST6Gal1) can be used to transfer functionalized sialic acid to *N*-glycans. Li et al. incorporated 9-azido-*N*-acetylneuraminic acid to the Fc glycans of an anti-CD22 mAb and attached various labels and a cytotoxic drug by strain-promoted azide-alkyne cycloaddition.[15]

Another category of glycan-remodeling approaches involves the enzymatic trimming of the *N*-glycans at Asn297 to core GlcNAc residues using endo-β-*N*-acetylglucosaminidase S2 (Endo S2).[16–18] B4GalT1(Y289L) is then used to transfer *N*-azidoacetylgalactosamine to the core GlcNAc present at Asn297, which provides a handle for conjugation of payloads by copper-free click chemistry. This approach has been used extensively for the conjugation of cytotoxic drugs and fluorophores for imaging.[16–19] It will add one payload per *N*-linker glycan, giving a uniform drug-to-antibody ratio (DAR). The use of multivalent linkers can further increase the achievable DAR.[20] The strategy of transferring an azidosugar to the core GlcNAc has matured into two commercially available technologies for site-specific conjugation, GlycoConnect™ (SynAffix) and GlyCLICK® (Genovis).

Endoglycosidase-catalyzed glycan remodeling strategies can also use glycan oxazoline derivatives as the activated substrates to transfer functionalized glycans to the core GlcNAc at Asn297.[21] IgG glyco-engineering with endoglycosidases usually proceeds in two steps: deglycosylation by wild-type endoglycosidase and then transglycosylation by a mutated endoglycosidase. Recently, it was demonstrated that wild-type Endo-S2 has highly relaxed substrate specificity and can accommodate different types of disaccharide oxazolines for transglycosylation to the core GlcNAc at Asn297.[22–24] This approach provided azide-tagged antibodies, which were readily clicked with payloads.

In all of the chemoenzymatic glycan remodeling strategies described above, the enzymes will modify the naturally occurring glycan residues found at Asn297. While this allows for site-specificity and reduction in heterogeneity, the proximity of this modification to the region of binding to Fc receptors could result in undesirable modifications of effector functions. While ST6Gal1 catalyzes the sialylation of *N*-linked glycans in both the Fc and Fab regions of antibodies, we found that certain bacterial sialyltransferases catalyze sialylation of *N*-linked glycans in the Fab region of antibodies, but not of *N*-linked glycans in the Fc region of antibodies (unpublished results). By exploiting these bacterial sialyltransferases, antibodies with at least one *N*-linked glycan in the Fab region may be modified to include a functionalized sialic acid in a site-specific manner while preserving antigen binding and Fc-dependent effector functions. Due to the biantennary structure of the glycans, each branch may contain one functionalized sialic acid residue, thus permitting up to 2 payload molecules to be conjugated per *N*-linked glycan. Further utility of this approach was demonstrated here by designing novel *N*-glycosylation sites in the Fab constant region of a model mAb (trastuzumab), which does not have a natural Fab glycan.

Results

Specific conjugation to the Fab glycan of cetuximab using a bacterial sialyltransferase (AST-03)

While testing various bacterial sialyltransferases for their ability to catalyze the addition of sialic acid to mAbs, we observed very little modification of the Fc glycans (data not shown). However, we noticed significant incorporation of sialic acid in the case of cetuximab and we hypothesized that these bacterial sialyltransferases may be selectively modifying the Fab glycans found in this antibody. We decided to focus on the α-2,3-sialyltransferase from *Actinobacillus suis* (open reading frame ASU2_08685) because it expressed very well as a fusion with the *Escherichia coli* maltose-binding protein (construct AST-03). The specificity of AST-03 for the transfer of α-2,3-linked sialic acid to terminal galactose was confirmed by NMR analysis of a synthetic sialyllactose derivative (data not shown). The ability of AST-03 to transfer sialic acid to cetuximab was first confirmed by isoelectric focussing gel analysis (Figure S1). The migration to more acidic forms was not as extensive with AST-03 as with ST6Gal1, which was consistent with additional site-specificity for AST-03. The specificity of AST-03 for the Fab glycan of cetuximab was later confirmed by mass spectrometry (MS) (data not shown and Figure S2). We used AST-03 to develop a strategy for the incorporation of *N*-azidoacetylneuraminic acid (Neu5NAz) specifically into the Fab glycans of mAbs (Figure 1). Once Neu5NAz is present in a glycan, a label or a drug can be easily covalently attached by click chemistry. In contrast, the mammalian sialyltransferase ST6Gal1 can modify both the Fc and the Fab glycans, which can potentially interfere with the effector functions that are dependent on the Fc glycans.

Cetuximab was first treated with a sialidase to remove the 2,3-linked sialic acids that are known to be present on the *N*-glycans of proteins produced in Chinese hamster ovary (CHO) cells.[25] In order to enhance the level of galactosylation, the material was also incubated with UDP-Gal and the B4GalT galactosyltransferase. After purification, cetuximab was modified by the addition of Neu5NAz using either AST-03 or ST6Gal1, followed by addition of MB488-DBCO using click chemistry. For comparison, cetuximab was also randomly labeled by conjugating the NHS ester of Alexa Fluor® 488 to

Table 1. Flow cytometry-derived apparent K_D determinations of fluorescently labeled cetuximab with EGFR-expressing SKOV3 and U87wtEGFR cells. Results are expressed as average ± stdev (n).

			Apparent K_D (nM)	
	Site	DOL	SKOV3	U87wtEGFR
NS Lys-AF488	Lys	5.1	No binding	No binding
cetux Lys-AF488	Lys	4.0	0.19 ± 0.01 (2)	1.69
cetux Fab-MB488	Fab	2.0	0.17 ± 0.03 (2)	1.66
cetux Fc/Fab-MB488	Fc/Fab	3.7	0.19 ± 0.02 (2)	1.66

Table 2. Glycoprofile of cetuximab labeled on Fab glycans with Neu5NAz using AST-03 and conjugated with MMAE (cetux Fab-vc-MMAE, see Figure S2A).

Region	Glycoform [a]	Relative abundance observed by MS (%)
Fc Glycan (Fc/2 fragment)		
	Man5	1
	$HexNAc_3Hex_4Fuc$	3
	A2G1	1
	FA2G1	26
	A2G2	6
	A2G2 + Hex [b]	7
	FA2G2	51
	FA2G2 + Hex [b]	2
	FA2G1 + Neu5NAz + MMAE	1
	FA2G2 + Neu5NAz + MMAE	1
Fab Glycan (Fd fragment)		
	FA2G2	11
	FA2G2 + Neu5NAz + MMAE	74
	FA2G2 + 2(Neu5NAz + MMAE)	15

[a]According to the Oxford notation (see Table S1 for detailed structures). Glycoform identities are based on mass.
[b]Additional hexose (Hex) is thought to be due to glycation of the Fc/2 fragment.

the primary amines (surface-accessible lysines). An antibody directed against a viral protein was used as a negative (non-specific, NS) control antibody, to determine levels of non-targeted binding. Flow cytometry was used to test cell surface binding of the glyco-conjugated cetuximab antibodies on SKOV3 cells naturally overexpressing the epidermal growth factor receptor (EGFR) and on U87 glioblastoma cells engineered to overexpress EGFR. Both types of glyco-conjugated cetuximab antibodies showed similar affinity for SKOV3 and EGFR-overexpressing U87 glioblastoma cells relative to the non-targeted antibody (Figure S3). Furthermore, anti-EGFR antibodies that were conjugated via their glycan residues (cetux Fab-MB488 and cetux Fc/Fab-MB488) were similar in binding affinity to target cells when compared to antibodies labeled on random lysine residues (Table 1).

Glycoprofile analysis of glyco-engineered cetuximab and of conjugates by liquid chromatography – mass spectrometry

MS analysis was used to determine the glycoprofile of cetuximab labeled on Fab glycans with Neu5NAz using AST-03 (Table 2, Figure S2A) and of cetuximab labeled with Neu5NAz on Fc/Fab using ST6Gal1 (Table 3, Figure S2B). The glyco-engineered cetuximab versions were conjugated by click chemistry with MMAE attached to a self-immolative linker terminated with dibenzocyclooctyne (DBCO-PEG4-vc-PAB-MMAE). To distinguish between Fab and Fc glycosylation, cetuximab was cleaved in the hinge region using the immunoglobulin-degrading enzyme from *Streptococcus pyogenes* (IdeS) and reduced into light chain, Fc/2 (with Fc glycan) and Fd fragments (with Fab glycan) prior to liquid chromatography (LC)-MS. For cetuximab modified using AST-03, 89% of the Fab glycoforms are modified with at least one MMAE molecule, while only 2% of the Fc glycoforms are modified with MMAE (Table 2). For cetuximab modified using ST6Gal1, the profile shows the opposite specificity: a greater percentage of Fc glycoforms are modified with MMAE than Fab glycoforms (Table 3). However, other experiments have determined that ST6Gal1 can also modify efficiently the Fab glycoforms (data not shown), i.e., ST6Gal1 is more promiscuous and does not generally display a preference toward the Fc glycans over the Fab glycans.

Growth inhibitory effect of glyco-engineered cetuximab conjugated with MMAE

We subsequently tested the effect of MMAE-conjugated cetuximab ADCs on the viability of U87 glioblastoma cells that overexpress EGFR (Figure 2, Table 4). A control experiment showed that unconjugated cetuximab had a much lower growth inhibition effect than the MMAE-conjugated cetuximab ADCs (Figure S4). As another negative control, cell viability due to a nonspecific ADC (NS ADC, directed against a viral protein) was tested to determine levels of non-targeted growth inhibition. All conjugated cetuximab antibodies were shown to be active in causing growth inhibition in EGFR-overexpressing U87 glioblastoma cells, resulting in at least 1000-fold increase in potency relative to the NS ADC. In particular, cetuximab antibodies that were conjugated to their glycan residues (cetux Fab-vc-MMAE, and cetux Fc/Fab-vc-MMAE) were more or as potent in their ability to cause growth inhibition as compared to antibodies labeled on random Cys residues (cetux Cys-vc-MMAE) (Figure 2a, Table 4) on an antibody/ADC molar basis. This effect was shown to be even more evident when ADC potency was calculated based on the drug added (MMAE IC_{50}, Figure 2b, Table 4).

Specific conjugation to de novo N-glycosylation sites in the CH1 domain of Fab of trastuzumab

While IgA2, IgE and IgM have naturally occurring Fab glycosylation sites,[26] only ~20% of human IgG1 antibodies have naturally occurring Fab glycosylation sites.[27,28] Cetuximab has a site within framework 3 of the variable portion of the heavy chain[29] and as such has two Fab *N*-glycosylation sites (one per heavy chain), whereas trastuzumab has no naturally occurring Fab *N*-glycosylation sites. There are advantages to specifically introducing glycosylation sites in the CH1 domain of mAbs. These advantages include portability across the IgG subclasses irrespective of the nature of the Fv with its antigen-binding complementarity-determining regions and remote location from the Fv and Fc regions, providing minimal interference with binding events to antigen and Fc receptors, respectively. The main aspects of the structure-based design of de novo glycosylation sites within CH1 focus on providing significant surface exposure of the glycosylation sequon, as well

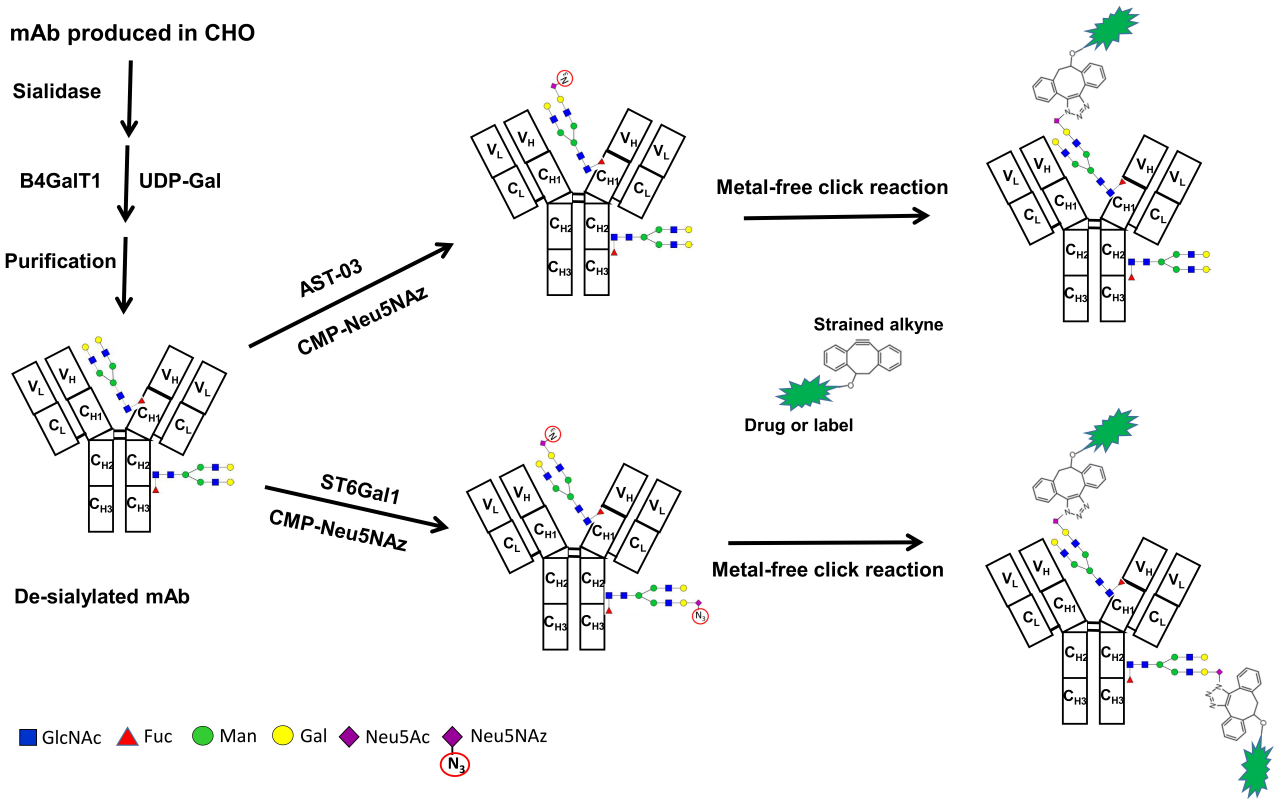

Figure 1. Overview of the conjugation to antibody glycans using sialyltransferases with different specificities. The mAbs are produced in CHO cells and a sialidase is used to remove the sialic acids (Neu5Ac) while the B4GalT1 galactosyltransferase is used to increase the presence of terminal β-1,4-linked galactose residues. Neu5NAz is transferred to the Fc and Fab glycans using ST6Gal1 or specifically to the Fab glycan using a bacterial sialyltransferase (AST-03). A label or a drug can then be covalently attached to the functionalized sialic acid (Neu5NAz). For simplicity, the *N*-glycans are depicted on one heavy chain monomer only.

Table 3. Glycoprofile of cetuximab labeled with Neu5NAz on Fc/Fab using ST6Gal1 and conjugated with MMAE (cetux Fc/Fab-vc-MMAE see Figure S2B).

Region	Glycoform [a]	Relative abundance observed by MS (%)
Fc Glycan (Fc/2 fragment)		
	Man5	2
	Man6	1
	A2G1	1
	FA2G1	17
	A2G2	1
	FA2G2	5
	FA2G1 + Neu5NAz	1
	FA2G2 + Neu5NAz	7
	FA2G1 + Neu5NAz + MMAE	9
	FA2G2 + Neu5NAz + MMAE	32
	FA2G2 + 2(Neu5NAz + MMAE)	18
	FA2G2 + Neu5NAz + MMAE + Hex [b]	2
	FA2G2 + (Neu5NAz + MMAE) + NeuAc5NAz	4
Fab Glycan (Fd fragment)		
	FA2G2	95
	FA2G2 + Neu5NAz + MMAE	5

[a]According to the Oxford notation (see Table S1 for detailed structures). Glycoform identities are based on mass.
[b]Additional hexose is thought to be due to glycation of the Fc/2 fragment.

as minimal change in stability upon introduction of the sequon and the attached carbohydrate moiety. Molecular modeling was used to determine appropriate sites for introduction of novel *N*-linked glycosylation sites in trastuzumab. The structural template for molecular design was based on a typical crystallographic structure of a Fab at high resolution. The selection criteria for de novo glycosylation sites were as follows: (1) NX(T/S) sequon is introduced by a single mutation; (2) Single mutation adds N residue not T/S residue in order to limit modifications to a single position (i.e., if T/S is mutated, then both N and T/S positions are modified); (3) mutation to N residue does not replace hydrophobic residues L, I, V, M, and F; (4) mutation to N residue does not replace conformationally special residues P and G; (5) side chain of wild-type residue to

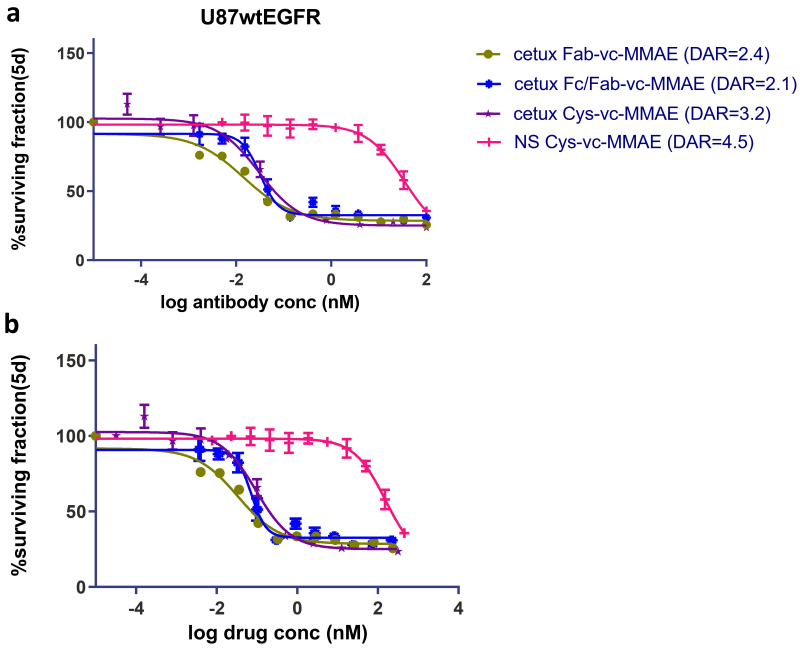

Figure 2. Growth inhibitory effect of glyco-engineered cetuximab conjugated with MMAE in U87 glioblastoma cancer cells engineered to overexpress EGFR. Potency was determined according to concentration of antibody (Panel **a**) or MMAE drug (Panel **b**).

Table 4. Growth inhibition potency of cetuximab ADCs in EGFR overexpressing U87 glioblastoma cells.

ADC	Drug site	DAR	ADC IC_{50} (nM) [a]	MMAE IC_{50} (nM) [b]
NS Cys-vc-MMAE	Cys	4.5	34	155
cetux Cys-vc-MMAE	Cys	3.2	0.03	0.095
cetux Fab-vc-MMAE	Fab	2.4	0.014	0.03
cetux Fc/Fab-vc-MMAE	Fc/Fab	2.1	0.032	0.07

[a]IC_{50} calculations are based on antibody-drug conjugate concentrations.
[b]IC_{50} calculations are based on drug concentrations.

be mutated is surface exposed; (6) side chain of wild-type residues to be mutated is not engaged in significant hydrophobic contacts or hydrogen bonds with other atoms of the mAb; (7) side chain of wild-type residue to be mutated is not part of α-helix or β-strand secondary structure elements; (8) introduced N residue side chain can adopt a conformation that projects the side-chain nitrogen atom toward the solvent; (9) *N*-linked monosaccharide GlcNAc can adopt a conformation that does not clash with atoms of the mAb and is projected toward the solvent; (10) *N*-linked monosaccharide GlcNAc is at least 15 Å away from the nearest atom in the variable domain; and (11) de novo glycosylation sites are at least 15 Å away from each other (defined as the distance between Cα atoms of the residues mutated to N residues).

The sites designed according to the selection criteria listed above are highlighted in the sequence alignment (Figure S5A) between the wild-type CH1 domain of the human IgG1, its single-point mutants introducing glycosylation sites at three positions, i.e., K129N, A158N, and T191N, and double and triple combinations thereof. Selected sites for de novo glycosylation appear to be well conserved among the CH1 domains of other human IgG isoforms according to a sequence alignment (Figure S5B). For comparison, we included as a control a published engineered *N*-glycosylation site that was designed in the heavy constant domain of a humanized anti-CD22 mAb, hLL2.[30] The specific mutation of this construct (hLL2HCN5) corresponds to L189N in trastuzumab (see sequential residue numbering in Table S2).

Figure 3 shows the location of the de novo glycosylation sites highlighted on a typical Fab crystal structure of high resolution (PDB code 3MXW at 1.8 Å resolution, heavy chain in black, light chain in white rendering). Geometric measurements indicated that the distances between the alpha carbon atoms of the residues mutated to asparagine residues are larger than 15 Å, and each site is over 20 Å from at least another site. This is important in order to avoid overcrowding of glycan residues and excessive hydrophobicity upon drug linkage to multiple de novo sites simultaneously. The distance between modeled *N*-linked monosaccharides GlcNAc at the de novo sites and the variable domain is at least 19 Å. This advantageously ensures a minimal impact of the carbohydrate-linked drug on the variable domain bearing the antigen binding affinity determinants. The wild-type residues mutated to the asparagines of the de novo sites are weakly involved in intramolecular interactions within the Fab. This is suggestive of negligible structural and stability changes upon introduction of these de novo glycosylation sites. The atomic environments around each wild-type mutated residue are shown in Figure S6.

Three *N*-linked glycosylation sites were engineered (individually) in the Fab of trastuzumab. The constructs were

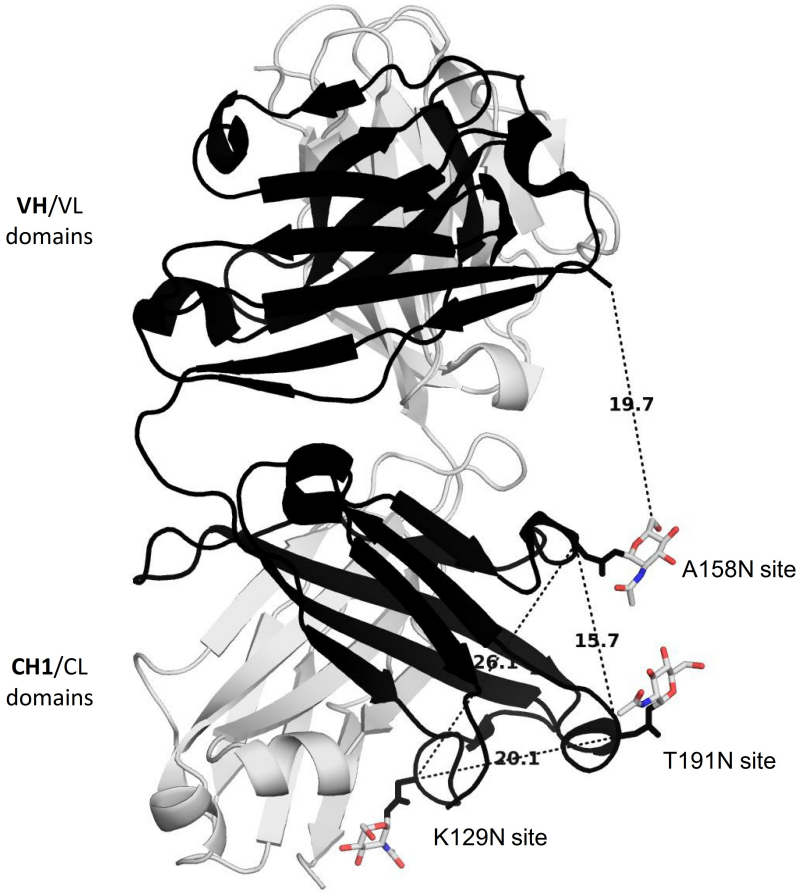

Figure 3. The locations of the de novo glycosylation sites are highlighted on a typical Fab crystal structure of high resolution (PDB code 3MXW at 1.8 Å resolution, heavy chain in black, light chain in white rendering). Shown distances are in Ångstrom units.

expressed in CHO cells. MS analysis shows that each site is fully occupied by glycans (Figure S7). The three single *N*-linked mutants were combined in pairs and as a triple Fab mutant in trastuzumab. The double mutants and the triple mutant are shifted even more toward the positive electrode (anode) than a single mutant control (L189N) on an isoelectrofocusing gel stained with Coomassie blue (Figure S8). This shift to more acidic forms confirms that the double and triple mutants have more sialylated *N*-glycans and consequently more sites for incorporation of Neu5NAz, which could result in DAR increases.

Modulation of the DARs could be obtained by removing the Neu5Ac with a sialidase and introducing Neu5NAz using AST-03. Figure S9 shows the shift toward the anode when there are additional introduced *N*-linked sites and following incubation of de-sialylated and galactosylated trastuzumab mutants with AST-03 and CMP-Neu5NAz. The distributions of isoelectric forms are also more uniform than the material before glycan remodeling (see Figure S8 versus Figure S9), suggesting that modulation of DARs could be uniform.

Target binding of glyco-engineered trastuzumab mutants by flow cytometry

Labeling of glyco-engineered trastuzumab mutants with MB488-DBCO resulted in a stoichiometry or degree of labeling (DOL) that correlated directly with the number of de novo glycosylation sites present in the antibodies for the single (DOL from 2.2 to 2.5) and double-conjugation site variants (DOL from 3.6 to 4.4) as indicated in Table 5. Trastuzumab with three de novo glycosylation sites had a DOL of 5.1, which was similar to that obtained with labeling of random Lys (trast Lys) that resulted in a DOL of 5.2. Notably, the wild-type antibody modified on the naturally occurring Fc glycosylation (Asn297) site using ST6Gal1 (trast Fc) had a DOL of 1.5, which is lower than any of the corresponding Fab conjugates modified on de novo Fab sites with AST-03. Cell-surface binding of glyco-conjugated trastuzumab antibodies were tested on human epidermal growth factor receptor 2 (HER2)-expressing SKBr3 and SKOV3 cells by flow cytometry (Figure S10). Antibodies containing de novo glycosylation sites were compared to those labeled on the Fc site Asn297 (trast Fc), as well as those labeled on random lysine residues (trast Lys). As a negative control, binding of an irrelevant nonspecific antibody (NS Lys) was tested to determine levels of nonspecific binding. Generally, the levels of median fluorescence intensity (MFI) at antibody saturation (Bmax) correlated well with the DOL, suggesting that the sites of conjugation did not significantly affect antigen binding. On all cell lines tested, cell surface-binding affinities (apparent K_D) were comparable amongst all the single-site conjugates tested (ranging from 1.8 to 2.7 nM for SKBr3 and 2.5–3.7 for SKOV3, see Table 5) and slightly stronger than that of Lys-conjugated trastuzumab. Cell binding affinities of the double and triple mutants were only slightly weaker than that

Table 5. Flow cytometry derived apparent K_D determinations of MB488-labeled glyco-engineered trastuzumab variants with HER2-expressing cell lines.

			Apparent K_D (nM)	
	Site	DOL	SKOV3	SKBr3
NS Lys	Lys [a]	5.1	No binding	No binding
trast Lys	Lys [a]	5.2	4.6	2.9
trast Fc	Fc	1.47	2.5	2.0
trast-L189N	Fab	2.35	3.5	2.7
trast-A158N	Fab	2.5	3.5	2.6
trast-K129N	Fab	1.74	2.5	2.3
trast-T191N	Fab	2.23	3.7	1.8
trast-K129N/A158N	Fab	4.02	7.1	4.5
trast-K129N/T191N	Fab	4.37	10.8	5.9
trast-A158N/T191N	Fab	3.58	4.0	2.6
trast-K129N/A158N/T191N	Fab	5.13	8.9	4.5

[a]The Lys were labeled with AF488.

of the corresponding single mutants with the exception of the A158N/T191N double mutant, whose apparent K_D was in the range obtained with the single mutants.

Glycoprofile analysis by LC-MS of glyco-engineered trastuzumab and its mutants conjugated with MMAE

MS analysis was used to determine the glycoprofile of wild-type trastuzumab (trast-WT) labeled with Neu5NAz using ST6Gal1 and trastuzumab selected single mutants (trast-A158N, trast-L189N and trast-T191N) labeled with Neu5NAz using AST-03, and subsequently conjugated with MMAE (Figure S11). The glycoforms observed are detailed in Tables 6 and 7 below. Only trast-WT, which only has an Fc glycosylation site and was treated with ST6Gal1, showed any Neu5NAz-MMAE labeling of the Fc glycan (Table 6). For the mutants treated with AST-03, only the Fab glycan was modified with Neu5NAz + MMAE (Tables 6 and 7). For each of the mutants, the majority of Fab glycoforms have at least one MMAE attached.

Growth inhibitory effect of glyco-engineered trastuzumab conjugated with MMAE

The ability of glyco-conjugated trastuzumab mutant antibodies to inhibit the growth of HER2-expressing SKOV3 cells was compared to that of trastuzumab labeled on random cysteines. As a negative control, an irrelevant nonspecific antibody (NS antibody Cys-vc-MMAE) was tested to determine levels of

Table 6. Glycoprofile of Fc (Fc/2 fragment) of glyco-engineered trastuzumab variants after clicking with DBCO-PEG4-vc-PAB-MMAE (see Figure S11).

	Relative abundance observed by MS (%)			
Glycoform [a]	trast-WT	trast-A158N	trast-L189N	trast-T191N
Man5	8	0	3	0
Man6	0	0	1	0
$HexNAc_3Hex_4Fuc$	0	3	3	3
FA2	2	1	0	0
FA2G1	22	40	34	42
$HexNAc_5Hex_3Fuc$	4	0	0	0
FA2G2	2	56	58	54
FA2G1 + Neu5NAz + MMAE	21	0	0	0
FA2G2 + Neu5NAz + MMAE	13	0	0	0
FA2G2 + 2(Neu5NAz + MMAE)	19	0	0	0
FA2G1 + Neu5NAz + MMAE − 762 Da	5	0	0	0
FA2G2 + 2(Neu5NAz + MMAE) − 762 Da	5	0	0	0

[a]According to the Oxford notation (see Table S1 for detailed structures), Glycoform identities are based on mass.

Table 7. Glycoprofile of Fab (Fd fragment) of glyco-engineered trastuzumab variants after clicking with DBCO-PEG4-vc-PAB-MMAE (see Figure S11).

	Relative abundance observed by MS (%)			
Glycoform [a]	trast-WT	trast-A158N	trast-L189N	trast-T191N
None	100	0	0	0
FA2G1	0	0	0	0
FA2G2	0	16	10	17
FA3G3	0	1	0	0
FA2G2 + Neu5NAz + MMAE	0	52	59	45
FA2G2 + Neu5NAz + MMAE − 762 Da	0	17	17	21
FA3G3 + Neu5NAz + MMAE	0	14	13	15
FA2G2 + 2(Neu5NAz + MMAE)	0	0	0	1

[a]According to the Oxford notation (see Table S1 for detailed structures). Glycoform identities are based on mass.

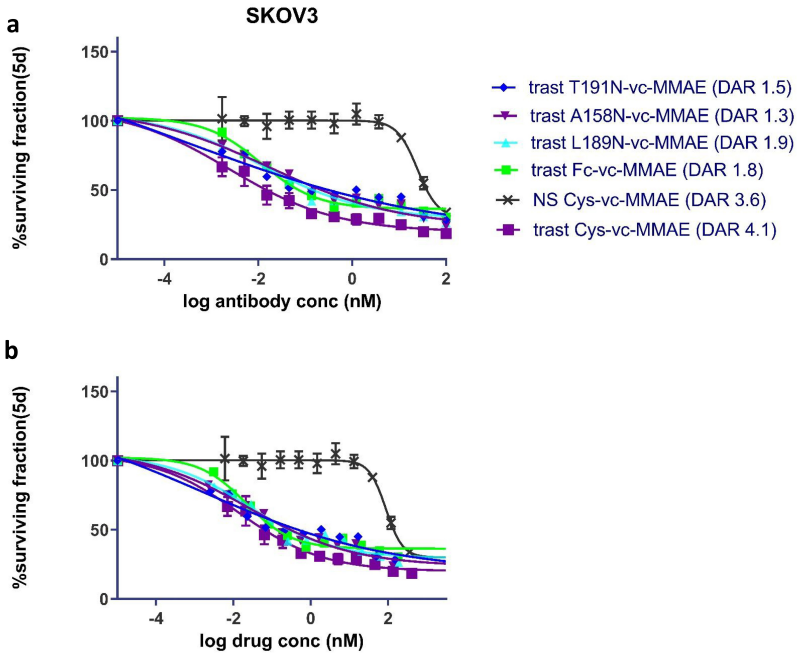

Figure 4. Growth inhibitory effect of glyco-engineered wild-type trastuzumab and designed single mutants conjugated with MMAE in HER2-expressing SKOV3 cells. Potency was determined according to molar concentration of antibody (Panel **a**) or MMAE (Panel **b**) component.

Table 8. IC_{50} determinations of MMAE-glyco-engineered trastuzumab in HER2 overexpressing SKOV3 ovarian cancer cells.

	Drug site	DAR	ADC IC_{50} (nM) [a]	MMAE IC_{50} (nM) [b]
trast Fc-vc-MMAE	Fc	1.8	0.01	0.02
trast A158N-vc-MMAE	Fab	1.3	0.02	0.02
trast L189N-vc-MMAE	Fab	1.9	0.01	0.02
trast T191N-vc-MMAE	Fab	1.5	~0.01	~0.02
trast Cys-vc-MMAE	Cys	4.1	0.002	0.01
NS Cys-vc-MMAE	Cys	3.6	24.6	87.9

[a]IC_{50} calculations are based on antibody-drug conjugate concentrations.
[b]IC_{50} calculations are based on drug concentrations.

nonspecific growth inhibition activity. All conjugated trastuzumab antibodies were shown to be active in causing growth inhibition of HER2 overexpressing SKOV3 ovarian cancer cells relative to the non-targeted ADC, NS Cys-vc-MMAE. Trastuzumab mutants conjugated at de novo glycosylation sites in the CH1 domain had comparable growth inhibition activity to antibodies glyco-conjugated in the Fc domain (Figure 4a, Table 8). This was also shown to be the case when ADC potency was calculated on the concentration of the drug added (Figure 4b, Table 8). However, the trastuzumab control that was randomly labeled on Cys (trast Cys-vc-MMAE) had a significantly lower ADC IC_{50} because of its higher DAR. When corrected for this factor, the drug-based IC_{50} (MMAE IC_{50}) were similar for the randomly labeled trastuzumab and the trastuzumab versions labeled on the glycans.

Discussion

Using glycans as "handles" for conjugation is an attractive method to achieve site-specificity without compromising target binding, potentially allowing the development of conjugated antibodies with optimal functional and biophysical properties. There are multiple strategies available to introduce a reactive group to Fc glycans or to both Fab and Fc glycans. Using a previously undescribed bacterial sialyltransferase, AST-03, we have developed a novel method to incorporate functionalized sialic acids specifically into the Fab glycans of mAbs. By directing conjugation specifically to only the Fab glycan, we can avoid interfering with effector functions that are dependent on the Fc glycans. However, other studies have found benefit to the reduction or inactivation of interaction with Fc-γ-receptors and/or mannose receptors to potentially reduce off-target uptake and cytotoxicity.[17] It remains to be determined which therapeutic applications would benefit the most from having intact Fc glycans on mAbs carrying cytotoxic (or other types of) payloads.

Significant glycan heterogeneity is still present when using the method targeting the Fab glycans with AST-03 (Tables 2, 6 and 7). Since this method does not modify the Fc glycans, the glycan heterogeneity present at that site will remain after the glycan remodeling and conjugation process. The glycan heterogeneity at the Fab glycan is mostly derived from the variability of conjugated drug molecules as the main glycoform is FA2G2 (Tables 2 and 7). Since the mAbs were produced in CHO cells, it should be noted that the observed glycan heterogeneity of cetuximab used in this work was lower than for cetuximab produced in the SP2/0 murine myeloma cell line.[29,31] *N*-glycans in cetuximab derived from the SP2/0 murine myeloma cell line

can be terminated with one or two α1,3 Gal epitopes increasing the complexity of the glycans and potentially causing anaphylaxis in patients. Although the literature reports that low levels of terminal α1,3 Gal epitopes are possible in CHO cells, they are generally very low or almost absent in many CHO cell lines, including the one used in this work.[25,32,33]

The specificity of the bacterial sialyltransferase AST-03 for the Fab glycan was first demonstrated with cetuximab, which has a naturally occurring Fab glycan. Using MS, we confirmed that the cytotoxin was attached to Neu5NAz that was transferred to the Fab glycan only (Table 2 and Figure S2A) when AST-03 was used for the glycan remodeling, and to the Fc and Fab glycans when ST6Gal1 was used (Table 3 and Figure S2B). The glyco-engineered cetuximab ADCs had similar growth inhibition potencies as the cetuximab ADC with drug conjugated to random Cys residues (Figure 2 and Table 4). Our proposed glycan remodeling method is limited in being directly usable only for the 20–25% of the mAbs that have a Fab glycan, whereas the conjugation methods based on the conserved Fc glycan can be universally used. However, we have further expanded the utility of Fab specific glycan remodeling by designing de novo Fab *N*-glycosylation sites in trastuzumab. Again, the growth inhibition potencies were similar when comparing the glyco-engineered versions with the trastuzumab ADC conjugated to random Cys residues (Figure 4 and Table 8). The data obtained with the two antibodies under study demonstrate that ADCs formed through glycan remodeling and conjugation are as potent as ADCs generated through more conventional random cysteine conjugation, while also achieving better site specificity.

Here, we report DARs in the range of 2.1–2.4 for the conjugation of MMAE to the cetuximab versions obtained by glycan remodeling (Table 4), while the DAR range was 1.3–1.9 for the trastuzumab single-point mutant versions (Table 8). MS showed that the main observed *N*-linked glycoform was FA2G2, a biantennary structure with core fucosylation (Tables 2, 3, 6and 7). The two terminal galactose residues (one on each branch) provide acceptor sites for the transfer of two Neu5NAz on each *N*-glycan. Complete occupancy would imply four added Neu5NAz for the Fab glycans (with one biantennary *N*-glycan per heavy chain) and eight added Neu5NAz for modification of Fc/Fab glycans (with two biantennary *N*-glycans per heavy chain). Although FA2G2 is the main glycoform, under-galactosylated glycoforms (FA2G1) are still present in the Fc glycan (Tables 2, 3 and 6). This happened even if we included a step (incubation with β-1,4-galactosyltransferase and UDP-Gal) for getting as complete galactosylation as possible. We have been able to achieve higher DARs than those reported in this study by increasing the enzyme loadings (for both the galactosyltransferase and the sialyltransferase) and using longer incubation times (data not shown). It is likely that desired DARs in the range of 2–4 can be achieved by modulating the incubation times and enzyme loadings.

The three *N*-linked glycosylation sites that were engineered individually into the Fab of trastuzumab were shown to be fully occupied by *N*-glycans when produced in CHO cells (Figure S7). These glycans provided "acceptor ends" for the attachment of Neu5NAz using AST-03, which enables the use of our protocol for specifically adding a cargo to the Fab region of the modified trastuzumab versions. The locations of the engineered *N*-linked glycosylation sites were in the constant domain and selected to minimize the impact of the introduced glycans on the variable domain bearing the antigen binding affinity determinants (Figure 3). This design and the proof-of-concept demonstration with trastuzumab suggest that these engineered *N*-glycosylation sites should be transferable to other IgGs that do not have Fab glycans. Moreover, our results indicate that these sites can be combined to generate higher stoichiometry labeling as needed. Affinity of the double and triple mutants was only slightly weaker than that of the corresponding single mutants (Table 5). Combining these sites could be used as a strategy to achieve higher DARs for increased potency or higher DOL in the case of imaging applications.

The protocols described here could also enable the conjugation of two different cargos, one to the Fab glycans and the other to the Fc glycans, providing a workflow to perform double-labeling in a site-directed manner. Double-labeling methods can also be based on the use on multivalent linkers. For instance, Adumeau et al. have synthesized a trivalent imaging probe bearing a near-infrared fluorophore, a radionuclide-chelating agent and an azide-reactive bicyclononyne that was conjugated to trastuzumab that had an azidosugar attached to the Fc glycan.[19] However, our method would allow for double-labeling of the same antibody at different specific sites, which could be advantageous for conjugating distinct payloads that are bulky or hydrophobic, or that cannot be directly attached the same backbone molecule. Another site-specific chemoenzymatic method was reported to be able to remodel separately the Fab and Fc *N*-glycans of cetuximab.[34] This method exploits the substrate specificity of three endoglycosidases (Endo-S, Endo-S2, Endo-F3 and their corresponding glycosynthase mutants) together with the site-selectivity of an α1,6-fucosidase from *Lactobacillus casei*. Using this strategy, heterogenous Fab *N*-glycans were replaced with a single sialylated *N*-glycan while the core fucosylated Fc *N*-glycans were remodeled with a fully galactosylated and non-fucosylated *N*-glycan. So far, there has been no report of this method being used for the conjugation of drugs or labels specifically to the Fab glycans, although the protocol would allow the introduction of payloads. As far as achieving specificity for the Fab region, the bacterial sialyltransferase reported in this work would have the benefit of introducing directly a functionalized sialic to the termini of the Fab glycans and allowing a more straightforward workflow for conjugation.

In conclusion, we have developed a novel method to incorporate functionalized sialic acids in the Fab glycans of mAbs. This method provides a workflow to improve homogeneity of conjugated cargos and generate ADCs without affecting the target specificity while preserving effector functions that are dependent on the Fc glycan.

Materials and methods

Production and purification of AST-03

A synthetic gene corresponding to the sequence of open reading frame ASU2_08685 (GenBank Accession # AFU19871)

from *A. suis* was ordered from Eurofins MWG Operon and delivered as an insert in plasmid pEX-K4. The insert was amplified using the Phusion® High-Fidelity DNA polymerase (New England Biolabs Inc.) and the primers AS-01 (5' CGTAGCGATA*CATATG*GAAAGAACCCCCCAACTAC 3', 35 mer, *Nde*I site in italics) and AS-02 (5' CTGAAG*GTCGAC*ATTATGAGGACAAACTACAATAATAC 3', 38 mer, *Sal*I site in italics). The PCR product was digested with *Nde*I and *Sal*I and cloned in pCWori+(*-lacZ*) containing the sequence encoding the *E. coli* maltose-binding protein (without the leader peptide) and the thrombin cleavage site, giving construct AST-03. *E. coli* AD202 containing construct AST-03 was grown in 2 YT medium containing 150 µg/mL ampicillin and 2 g/L glucose. The culture was incubated at 37°C until A_{600} = 0.5, induced with 1 mM IPTG, and then incubated overnight at 25°C. The cells were broken using an Avestin C5 Emulsiflex cell disruptor (Avestin) and the AST-03 sialyltransferase was purified by affinity chromatography on amylose resin following the manufacturer's instructions (New England Biolabs). The activity of the purified AST-03 α-2,3-sialyltransferase was measured using 0.5 mM 6-(5-fluorescein-carboxamido)-hexanoic acid succinimidyl ester (FCHASE)-labeled LacNAc, 0.5 mM CMP-Neu5Ac, 10 mM $MnCl_2$ and 50 mM Hepes pH 7 in a 5 min assay at 37°C. The samples were analyzed by capillary electrophoresis (CE) as described previously.[35] Quantitation of the reactions was performed by integration of the CE trace peaks using the MDQ 32 Karat software (Beckman, CA). One unit of activity was defined as the amount of enzyme that produces one µmol of Neu5Ac-LacNAc-FCHASE in 1 min.

Production and purification of ST6Gal1

ST6Gal1 was produced and purified as previously described.[36] In summary, the codon-optimized (human codon bias) gene encoding the human ST6Gal1 protein (GenBank accession # P15907) intralumenal domain (aa 27–406) with a human VEGFa (GenBank accession # P15692) signal peptide linked at its N-terminus and a C-terminal GHHHHHHHHHHG tag at its C-terminus was chemically synthesized by GenScript (Piscataway) and cloned into the pTT5® mammalian expression vector. The secreted ST6Gal1 enzyme was expressed in CHO-EBNA1 (CHO-3E7) cells and the clarified culture medium supernatant was harvested at 8 days post-transfection and the secreted ST6Gal1 was purified by immobilized metal-affinity chromatography.

Production and purification of cetuximab and trastuzumab variants

Codon-optimized (CHO codon bias) genes encoding the antibodies light and heavy chains were synthesized by GenWiz (Piscataway) and cloned into the pTT5® mammalian expression vector. The pTT5-HC and pTT5-LC plasmids were co-transfected at a ratio of 1:1 (w:w) in CHO-EBNA1 (CHO-3E7) cells grown in F17 medium using PEIMax as described previously and the clarified culture medium supernatant were harvested at 8 days post-transfection.[37] The clarified supernatants were captured by Protein A affinity chromatography (MabSelect SuRe, Cytiva), eluted in 100 mM Citrate-Na pH 3.0 and buffer-exchanged in PBS.

Synthesis of CMP-Neu5NAz

N-azidoacetyl-D-mannosamine (ManNAz) was obtained from Sussex Research Laboratories. The synthesis of *N*-azidoacetylneuraminic acid (Neu5NAz) was performed using a recombinant form of the Pm1715 sialic acid aldolase from *Pasteurella multocida*. The reaction mix with the Pm1715 sialic acid aldolase included 20 mM ManNAz, 100 mM sodium pyruvate and 100 mM Tris pH 8.6, and was incubated at 37°C for 18 h. The CMP-Neu5NAz was obtained by adding a recombinant form of the CMP-NeuAc synthetase from *Campylobacter jejuni* as well as 13 mM CTP (1:1 ratio in the diluted reaction) and 63 mM $MgCl_2$. The reaction was performed at 37°C for 1.5 h and the enzymes were removed by running the reaction mix on an Amicon Ultra-15 centrifugal filter unit with a 10,000 nominal molecular weight limit (NMWL). The filtrate was diluted 30-fold with water and applied to a 5 mL HiTrapQ HP column (7 runs total). The column was developed with a gradient of 0 to 0.25 M NH_4HCO_3 and the fractions containing CMP-Neu5NAz were identified by capillary electrophoresis analysis using a P/ACE MDQ system (Beckman Coulter) equipped with a diode array detector (electropherogram acquired at 271 nm). Capillaries were bare silica 50 µm × 60.2 cm with a detector at 50 cm, the running buffer was 25 mM sodium tetraborate, pH 9.4 and separations were performed at 27 kV for 30 min.

Remodeling of N-glycans on cetuximab

Sialic acid was removed by treating 9.6 mg of cetuximab with 0.96 unit of a recombinant sialidase from *Micromonospora viridifaciens* (construct MNV-02) for 2 h at 37°C in 50 mM Hepes pH 6.5. Removal of the sialic acid was confirmed by isoelectrofocusing using a PhastSystem (GE Healthcare Life Sciences), PhastGel IEF 3–9 and staining with Coomassie blue. The MNV-02 sialidase includes a 6-His tag and was removed by binding to 0.6 mL of Nickel Sepharose excel resin (GE Healthcare Life Sciences) while cetuximab was recovered in the flowthrough. An assay for sialidase activity measured residual activity, which required removal by binding of the cetuximab to a HiTrap Protein A column (GE Healthcare Life Sciences) as described below. In order to enhance the level of galactosylation, galactose was added using a recombinant version of the human B4GalT1 expressed in *E. coli*. The reaction mix included approximately 9 mg of de-sialylated cetuximab, 500 mU of B4GalT1, 10 mM $MnCl_2$, 10 mM UDP-Gal, 50 mM Hepes pH 6.5 and 100 mM NaCl. The reaction was performed at 37°C for 24 h. The cetuximab was purified by applying half of the reaction mix to a 1 mL Protein A column equilibrated with PBS buffer pH 7.5 (2 separate runs total were performed). The cetuximab was eluted with 100 mM citrate buffer pH 3 and the buffer was replaced with PBS pH 7.5 by desalting on a 5 mL HiTrap desalting column (GE Healthcare Life Sciences). The material was concentrated to 2.94 mg/mL (total of 7.64 mg recovered) using an Amicon Ultra-4 centrifugal filter unit with a 10,000 NMWL.

Addition of Neu5NAz to the Fab glycans of cetuximab

Neu5NAz was added to the Fab glycans of cetuximab using the AST-03 α-2,3-sialyltransferase. The reaction mix included 1 mg/mL de-sialylated and galactosylated cetuximab (total of 1.69 mg), 50 mM Hepes pH 7, 10 mM $MnCl_2$, 1 mM CMP-Neu5NAz and 55 mU of AST-03. The reaction was performed at 37°C for 21 h. The cetuximab(Fab-Neu5NAz) was purified by applying the reaction mix to a 1 mL Protein A column equilibrated with PBS buffer pH 7.5. The cetuximab(Fab-Neu5NAz) was eluted with 100 mM citrate buffer pH 3 and the buffer was replaced with PBS pH 7.5 by desalting on a 5 mL HiTrap desalting column (GE Healthcare Life Sciences). The material was concentrated to 2.64 mg/mL (total of 1.22 mg recovered) using an Amicon Ultra-4 centrifugal filter unit with a 10,000 NMWL.

Addition of Neu5NAz to the Fc and Fab glycans of cetuximab

Neu5NAz was added to the Fc and Fab glycans of cetuximab using ST6Gal1. The reaction mix included 1 mg/mL de-sialylated and galactosylated cetuximab (total of 3.1 mg), 50 mM Hepes pH 7.5, 10 mM $MnCl_2$, 1 mM CMP-Neu5NAz and 78 mU of ST6Gal1. The reaction was performed at 37°C for 24 h. The cetuximab (Fc/Fab-Neu5NAz) was purified by applying the reaction mix to a 1 mL Protein A column equilibrated with PBS buffer pH 7.5. The cetuximab (Fc/Fab-Neu5NAz) was eluted with 100 mM citrate buffer pH 3 and the buffer was replaced with PBS pH 7.5 by desalting on a 5 mL HiTrap desalting column (GE Healthcare Life Sciences). The material was concentrated to 2.84 mg/mL (total of 2.27 mg recovered) using an Amicon Ultra-4 centrifugal filter unit with a 10,000 NMWL.

Labeling of glyco-engineered cetuximab with MB488-DBCO

The glyco-engineered cetuximab (Fab-Neu5NAz) and cetuximab (Fc/Fab-Neu5NAz), both at 1.45 mg/mL (0.6 mg total), were reacted with 0.2 mM MB488-DBCO (Click Chemistry Tools) in PBS pH 7.4 for 24 h at 25°C in the dark. The unreacted MB488-DBCO was removed by loading the reactions on PD Miditrap G-25 columns (GE Healthcare Life Sciences) and eluting with PBS pH 7.5. The DOL was calculated using a molar extinction coefficient of 75,000 $M^{-1}cm^{-1}$ at 494 nm for MB488 and a correction factor of 0.26 at 280 nm. A molar extinction coefficient of 217,376 M^{-1} cm^{-1} at 280 nm for cetuximab was used. Pooling the most concentrated fractions yielded 0.31 mg of cetux Fab-MB488 with a DOL of 1.94, while the recovery for cetux Fc/Fab-MB488 was 0.38 mg with a DOL of 3.83. For comparison purposes, randomly labeled version of antibodies were generated by conjugated NHS ester (or succinimidyl ester) of Alexa Fluor® 488 to the primary amines (R-NH2) using conventional kits (ThermoFisher, Cat. No. A20000).

Click reactions of glyco-engineered cetuximab with DBCO-PEG4-vc-PAB-MMAE

The glyco-engineered cetuximab (Fab-Neu5NAz) at 1.86 mg/mL (0.65 mg total), was reacted with 0.13 mM DBCO-PEG4-vc-PAB-MMAE (Levena Biopharma) in 10% dimethylacetamide (DMA), 100 mM potassium phosphate, 20 mM NaCl, 2 mM EDTA, pH 7.2 for 24 h at 23°C in the dark. The glyco-engineered cetuximab (Fc/Fab-Neu5NAz) was reacted under the same conditions except that the concentration was 2 mg/mL (0.7 mg total) and the DBCO-PEG4-vc-PAB-MMAE concentration was 0.14 mM. The unreacted DBCO-PEG4-vc-PAB-MMAE was removed by loading the reaction on a 2 mL Zeba Spin Desalting column (Pierce) and eluting with 20 mM succinate, 0.02% Tween 20, pH 5.5, 6% trehalose. The desalting step was repeated for a total of three times. The DAR was calculated using molar extinction coefficients of 33,095 M^{-1} cm^{-1} at 248 nm and 7,615 M^{-1} cm^{-1} at 280 nm for clicked DBCO-PEG4-vc-PAB-MMAE. We used molar extinction coefficients 73,117 M^{-1} cm^{-1} at 248 nm of 210,863 M^{-1} cm^{-1} at 280 nm for cetuximab. The recovery was 0.47 mg of cetux Fab-vc-MMAE with a DAR of 2.4, while the recovery for cetux Fc/Fab-vc-MMAE was 0.57 mg with a DAR of 2.1.

Random conjugation of MC-vc-PAB-MMAE to Cys residues

For comparison purposes, vc-PAB-MMAE was randomly conjugated to reduced inter-chain Cys residues. Lyophilized MC-vc-PAB-MMAE was solubilized in DMA to a final concentration of 10 mM. The level of DAR is controlled by adjusting the degree of reduction of disulfide bonds by increasing the concentration of reducing agent. The reduction is initiated by the addition of Tris(2-carboxyethyl)phosphine from a 25X working stock into the antibody solution in the following buffer: 100 mM sodium phosphate, 20 mM NaCl, 2 mM EDTA, pH 7.2. The mixture is incubated at 37°C for 1 h. A 7.5-fold molar excess (100 μM) of MC-vc-PAB-MMAE is added to the reaction mixture from a 20X working stock in DMA. The final concentration of co-solvent in the reaction is 5% v/v. The reaction is incubated at 25°C for ~18 h. The following day, 5 mL 7 K MWCO Zeba Spin desalting columns (ThermoScientific, Cat. No. 89892) are pre-equilibrated in standard formulation buffer (20 mM Succinate, 0.02% w/v Polysorbate-20, pH 6.0). After the reaction is complete, Polysorbate-20 is added to a final concentration of 0.02% w/v prior to passing the reaction mixture consecutively through the pre-equilibrated Zeba columns. To the eluant, $1/5^{th}$ volume of 36% Trehalose solution (in formulations buffer) is added. Absorbance measurements of the conjugate at 248 nm and 280 nm were used to calculate the DAR, and the sample measured for monomeric purity by size-exclusion chromatography on a HPLC system using a Superdex 200 5/150 column (GE Healthcare Life Sciences).

Design of de novo glycosylation sites in the CH1 domain of Fab

The structural template for molecular design was based on a typical crystallographic structure of a Fab at high resolution. The crystal structure with ID code 3MXW solved at 1.8-Å resolution was retrieved from the Protein Data Bank (http://www.rcsb.org/). Structure examination was done using PyMol (The PyMOL Molecular Graphics System, Version 1.8 Schrödinger, LLC), including residue/side-chain surface exposure calculation,

secondary structure, polar contacts, hydrophobic neighboring residues, and distance measurements. Structural manipulation was done in Sybyl (Tripos, Inc.), including site residue mutagenesis, *N*-GlcNAc linkage and conformational analysis. Structural refinement was carried out with the Amber and Glycam force fields.[38,39] *N*-glycosylation scores were computed via the online server NetNGlyc 1.0.[40]

Removal of sialic acid from trastuzumab WT and mutants and addition of galactose

Sialic acid was removed by treating the trastuzumab variants (final concentration 1.3 mg/mL) with a recombinant sialidase (loading of 0.05 unit per mg of trastuzumab) from *M. viridifaciens* (construct MNV-02) for 2 h at 37°C in 50 mM Hepes pH 7. Galactose was added directly following the sialidase treatment using a recombinant version of the human B4GalT1 expressed in *E. coli*. The reaction was performed with 1 mg/mL of trastuzumab, B4GalT1 (loading of 0.04 unit per mg of trastuzumab), 10 mM $MnCl_2$, 10 mM UDP-Gal and 50 mM Hepes pH 7. The reaction was performed at 37°C for 18 h. The trastuzumab variants were purified by applying the reaction mix to a 1 mL Protein A column equilibrated with PBS buffer pH 7.5. The trastuzumab variants were eluted with 100 mM citrate buffer pH 3 and the buffer was replaced with PBS pH 7.5 by desalting on a 5 mL HiTrap desalting column (GE Healthcare Life Sciences). In some cases, the purified material was purified a second time on Protein A to remove residual sialidase activity. The purified de-sialylated and galactosylated trastuzumab variants were concentrated to between 1.5 and 2 mg/mL using an Amicon Ultra-4 centrifugal filter unit with a 10,000 NMWL.

Addition of Neu5NAz to the Fc glycans of trastuzumab WT

Neu5NAz was added to the Fc glycans of trastuzumab WT using ST6Gal1. The reaction mix included 1.22 mg/mL de-sialylated and galactosylated trastuzumab WT (total of 5.5 mg), 50 mM Hepes pH 7.5, 10 mM $MnCl_2$, 1 mM CMP-Neu5NAz and 137 mU of ST6Gal1. The reaction was performed at 37°C for 24 h. The trastuzumab WT (Fc-Neu5NAz) was purified by applying the reaction mix to a 1 mL Protein A column equilibrated with PBS buffer pH 7.5. The trastuzumab WT (Fc-Neu5NAz) was eluted with 100 mM citrate buffer pH 3 and the buffer was replaced with PBS pH 7.5 by desalting on a 5 mL HiTrap desalting column (GE Healthcare Life Sciences). The material was concentrated to 2.94 mg/mL (total of 4.33 mg recovered) using an Amicon Ultra-4 centrifugal filter unit with a 10,000 NMWL.

Addition of Neu5NAz to the Fab glycans of trastuzumab mutants

Neu5NAz was added to the Fab glycans of trastuzumab mutants using the AST-03 α-2,3-sialyltransferase. The reaction mixes included 0.83 to 1.17 mg/mL de-sialylated and galactosylated trastuzumab mutants (total of 2.75 to 6.46 mg depending on the mutant), 50 mM Hepes pH 7, 10 mM $MnCl_2$, 1 mM CMP-Neu5NAz and 10 mU of AST-03 per mg of trastuzumab mutant. The reaction was performed at 37°C for 18 h. The trastuzumab mutants (Fab-Neu5NAz) were purified by applying the reaction mixes to a 1 mL Protein A column equilibrated with PBS buffer pH 7.5. The trastuzumab mutants (Fab-Neu5NAz) were eluted with 100 mM citrate buffer pH 3 and the buffer was replaced with PBS pH 7.5 by desalting on a 5 mL HiTrap desalting column (GE Healthcare Life Sciences). The material was concentrated to 2.8 to 3.7 mg/mL (total of 2.7 to 5.3 mg recovered) using an Amicon Ultra-4 centrifugal filter unit with a 10,000 NMWL.

Labeling of glyco-engineered trastuzumab WT and mutants with MB488-DBCO

The glyco-engineered trastuzumab WT (Fc-Neu5NAz) and trastuzumab mutants (Fab-Neu5NAz), all at 1.45 mg/mL (1 mg total), were reacted with 0.2 mM MB488-DBCO (Click Chemistry Tools) in PBS pH 7.4 for 24 h at 25°C in the dark. The unreacted MB488-DBCO was removed by loading the reactions on PD Miditrap G-25 columns (GE Healthcare Life Sciences) and eluting with PBS pH 7.5. The DOL was calculated using a molar extinction coefficient of 75,000 M^{-1} cm^{-1} at 494 nm for MB488 and a correction factor of 0.26 at 280 nm. We used a molar extinction coefficient of 201,197 M^{-1} cm^{-1} at 280 nm for trastuzumab.

Click reactions of glyco-engineered trastuzumab WT and mutants with DBCO-PEG4-vc-PAB-MMAE

In order to increase the amount of incorporated Neu5NAz, a second reaction with either ST6Gal1 or AST-03 was performed as described above. The purified trastuzumab WT (Fc-Neu5NAz) and trastuzumab mutants (Fab-Neu5NAz) were purified as described above. The glyco-engineered trastuzumab WT (Fc-Neu5NAz) and trastuzumab single-site mutants (Fab-Neu5NAz) at 2 mg/mL (0.7 mg total), was reacted with 0.11 mM DBCO-PEG4-vc-PAB-MMAE (Levena Biopharma) in 10% DMA, 100 mM potassium phosphate, 20 mM NaCl, 2 mM EDTA, pH 7.2 for 24 h at 25°C in the dark. The unreacted DBCO-PEG4-vc-PAB-MMAE was removed by loading the reaction on a 2 mL Zeba Spin Desalting column (Pierce) and eluting with 20 mM succinate, 0.02% Tween 20, pH 5.5, 6% trehalose. The desalting step was repeated for a total of three times. The DAR was calculated using molar extinction coefficients of 33,095 M^{-1} cm^{-1} at 248 nm and 7,615 M^{-1} cm^{-1} at 280 nm for clicked DBCO-PEG4-vc-PAB-MMAE. We used molar extinction coefficients 81,973 M^{-1} cm^{-1} at 248 nm of 215,380 M^{-1} cm^{-1} at 280 nm for trastuzumab. The recoveries were in the range of 0.47 to 0.58 mg with DARs ranging from 1.33 to 1.88.

Glycoprofile analysis by LC-MS of glyco-engineered cetuximab, trastuzumab and of conjugates

Glycoprofile analysis by "Middle-up" LC-MS was performed as described in Raymond et al.[41] Light chain, Fc/2 (CH2-CH3) and Fd (VH-CH1) antibody fragments were obtained by digestion of the conjugated antibodies (20 µg, 2 mg/mL) with 20 U of "FabRICATOR" IdeS (Genovis) in 50 mM Tris-HCl pH 8 at

37°C for 30 min, followed by reduction with 20 mM DTT (Sigma) at 56°C for 30 min. The fragments were analyzed by LC-MS using an Agilent HP1100 Capillary LC system (Agilent Technologies) coupled to a LTQ-Orbitrap XL mass spectrometer (Thermo Fisher Scientific) equipped with a high-flow electrospray ionization source. 5 µg of digested antibody was loaded on a Poros R2 column (2.1 × 30 mm) (Applied Biosystems) heated to 80°C. Mobile phases were 0.1% formic acid in water (A) and 100% acetonitrile (B) preheated to ~80°C. A linear gradient of 10%-75% B over 12 min (3 mL/min) was used to desalt and partially resolve the Fc/2 and Fd fragments. The HPLC eluent was split to 100 µL/min just before the electrospray source of the LTQ-Orbitrap XL and MS spectra was acquired from *m/z* 400 to 2000 at a resolution of 15,000. LC-MS spectra were viewed in Xcalibur® (Thermo Fisher Scientific). Molecular weight profiles were generated with the MassLynx© MaxEnt1 deconvolution software (Waters). Databridge (Waters) was used to convert the protein LC-MS spectra into a format that was compatible with MaxEnt1. Identities were assigned to the glycosylated and conjugated antibody fragments based on the masses observed in the molecular weight profiles. The relative abundances listed in Tables 2,3, 6 and 7 were calculated on the basis of peak height. The apparent percentage of a given glycan was obtained as the signal height of the Fc/2 or Fd antibody fragments carrying this glycan divided by the total signal heights of all glycans for the same antibody fragment identified in the molecular weight profile.

Cell culture

For cetuximab conjugates, binding and functional testing was performed on cultured cells that are known to express the EGFR. U87wtEGFR glioblastoma cell lines were engineered to overexpress EGFR (provided by Web Cavanee).[42] For trastuzumab, binding and functional testing was performed on cultured cell that are known to express the HER2. SKOV3 (human ovarian adenocarcinoma) and SKBr3 (human breast carcinoma) cell lines were obtained from ATCC and cultured according to supplier's recommendations. Cells were passaged twice a week and used within 4–6 weeks for all cell lines.

Target binding by flow cytometry

Adherent cells were dissociated with non-enzymatic Sigma Cell Dissociation Solution (Cat. No. C5789). Cells suspensions were added to polypropylene, V-bottom 96-well plates and incubated for 2 h on ice with MB488- and AF488-labeled antibodies at concentrations ranging from 100 nM to 0.05 nM. After incubation, the cells were washed twice and resuspended in propidium iodide solution (10 µg/mL) to assess the viability. Data acquisition was performed the same day in the LSR-Fortessa Flow cytometer (Beckton Dickinson) equipped with fluorescence-activated cell sorting (FACS) Diva Software and HTS unit (automated sampling in 96-well plates). FACS data were exported into Excel data files and MFI (median fluorescence intensity) of the MB488- and AF488-stained, alive (single cells) peak was taken for calculations. Background subtraction was calculated for all wells using the MFI values of the cells incubated in the absence of antibodies. Background subtracted data were analyzed in GraphPad 6.0 using the one site-specific binding with Hill slope non-linear regression curve fit model to determine apparent Bmax and K_D for each of the test articles.

Growth Inhibition assay

Drug-conjugated cetuximab versions were tested for their effects on viability on glioblastoma cell lines that were engineered to overexpress EGFR (U87wtEGFR). Cells were seeded at 500 cells/well in 384-well plates (Corning® 384 Well White Flat Bottom Polystyrene TC-Treated Microplates, Cat. No. 3570). Drug-conjugated trastuzumab versions were tested for their effects on viability on HER2 overexpressing SKOV3 ovarian cancer cells. SKOV3 cells were seeded at 200 cells/well 384-well plates. Cells were allowed to grow for five days in the presence of serial dilutions of the test articles or benchmark controls ranging from 100 nM to 0.0017 nM. After five days (37°C, 5% CO_2, humidified incubator), the number of viable cells in culture was determined using CellTiterGlo (Promega), based on quantitation of the ATP present in each well, which signals the presence of metabolically active cells. Signal output was measured on a luminescence plate reader (Envision, Perkin Elmer) set at an integration time of 0.1 sec. Integration time is adjusted to minimize signal saturation at high ATP concentration. Each concentration point (S) was normalized to the negative control (NC) wells and expressed as % survival = (S × 100)/NC. Dose-response curves of % survival vs. log concentration were fit using GraphPad Prism 6.0 with a four-parameter logistic model to estimate IC_{50} and maximum efficacy (Model: Y = (Bottom+(Top-Bottom))/(1+ 〖10〗 ^((logIC50-X)×HillSlope))). IC_{50} is the concentration of agonist that gives a response half way between Bottom and Top. HillSlope describes the steepness of the curves. Top and Bottom are plateaus in the units of the Y axis.

Supporting information description

Supporting data: *N*-linked glycan structures according to Oxford notation (Table S1), residue numbering of trastuzumab mutations (Table S2), isoelectric focusing gel analysis (Figures S1, S8 and S9), MS analysis (Figures S2, S7 and S11), cell-binding assays (Figures S3 and S10), growth inhibitory effect (Figure S4), CH1 domain sequence alignments (Figure S5) and structural environments around CH1 sites selected for de novo glycosylation (Figure S6).

Abbreviations

ADC	Antibody-drug conjugate
AST-03	α-2,3-sialyltransferase from *Actinobacillus suis*
Cetux	Cetuximab
B4GalT1	β-1,4-galactosyltransferase 1
DAR	Drug to antibody ratio
DBCO	Dibenzocyclooctyne

DBCO-PEG4-vc-PAB-MMAE	MMAE drug with self-immolative linker (Val-Cit-PAB)
DMA	Dimethylacetamide
DOL	Degree of labeling
EGFR	Epidermal growth factor receptor
Fab	Fragment antigen-binding
Fc	Fragment crystallizable
Fd	Heavy chain region of the Fab
Fv	Variable domains of the light and heavy chains
HER2	Human epidermal growth factor receptor 2
Hex	Hexose
IdeS	Immunoglobulin-degrading enzyme from *Streptococcus pyogenes*
LC-MS	Liquid chromatography – mass spectrometry
MC-vc-PAB-MMAE	MMAE drug with maleimide and self-immolative linker (Val-Cit-PAB)
MFI	Median fluorescence intensity
MMAE	Monomethyl Auristatin E
Neu5NAz	*N*-azidoacetylneuraminic acid
NMWL	Nominal molecular weight limit
NS	Non specific
ST6Gal1	Sialytransferase ST6 β-galactoside α-2,6-sialyltransferase 1
Trast	Trastuzumab
WT	Wild type

Acknowledgments

We thank Frank St. Michael for help for the random conjugation of MC-vc-PAB-MMAE with cetuximab and trastuzumab. We also thank Denis L'Abbé for the production of the mAbs and Christian Gervais for the production of the ST6Gal1 sialyltransferase.

Disclosure statement

No potential conflict of interest was reported by the author(s).

Funding

This work was supported by the National Research Council Canada.

ORCID

Michel Gilbert http://orcid.org/0000-0002-0204-4408

References

1. Ducry L, Stump B. Antibody-drug conjugates: linking cytotoxic payloads to monoclonal antibodies. Bioconjugate Chem. 2010;21(1):5–13. doi:10.1021/bc9002019.
2. Panowski S, Bhakta S, Raab H, Polakis P, Junutula JR. Site-specific antibody drug conjugates for cancer therapy. MAbs. 2014;6(1):34–45. doi:10.4161/mabs.27022.
3. Junutula JR, Raab H, Clark S, Bhakta S, Leipold DD, Weir S, Chen Y, Simpson M, Tsai SP, Dennis MS, et al. Site-specific conjugation of a cytotoxic drug to an antibody improves the therapeutic index. Nat Biotechnol. 2008;26:925–32. doi:10.1038/nbt.1480.
4. Axup JY, Bajjuri KM, Ritland M, Hutchins BM, Kim CH, Kazane SA, Halder R, Forsyth JS, Santidrian AF, Stafin K, et al. Synthesis of site-specific antibody-drug conjugates using unnatural amino acids. Proc Natl Acad Sci U S A. 2012;109(40):16101–06. doi:10.1073/pnas.1211023109.
5. Italia JS, Addy PS, Erickson SB, Peeler JC, Weerapana E, Chatterjee A. Mutually orthogonal nonsense-suppression systems and conjugation chemistries for precise protein labeling at up to three distinct sites. J Am Chem Soc. 2019;141(15):6204–12. doi:10.1021/jacs.8b12954.
6. Hutchins BM, Kazane SA, Staflin K, Forsyth JS, Felding-Habermann B, Schultz PG, Smider VV. Site-specific coupling and sterically controlled formation of multimeric antibody Fab fragments with unnatural amino acids. J Mol Biol. 2011;406(4):595–603. doi:10.1016/j.jmb.2011.01.011.
7. Strop P, Liu SH, Dorywalska M, Delaria K, Dushin RG, Tran TT, Ho WH, Farias S, Casas MG, Abdiche Y, et al. Location matters: site of conjugation modulates stability and pharmacokinetics of antibody drug conjugates. Chem Biol. 2013;20(2):161–67. doi:10.1016/j.chembiol.2013.01.010.
8. Wu KL, Yu C, Lee C, Zuo C, Ball ZT, Xiao H. Precision modification of native antibodies. Bioconjugate Chem. 2021;32(9):1947–59. doi:10.1021/acs.bioconjchem.1c00342.
9. Okeley NM, Toki BE, Zhang X, Jeffrey SC, Burke PJ, Alley SC, Senter PD. Metabolic engineering of monoclonal antibody carbohydrates for antibody-drug conjugation. Bioconjugate Chem. 2013;24(10):1650–55. doi:10.1021/bc4002695.
10. Zhou Q, Stefano JE, Manning C, Kyazike J, Chen B, Gianolio DA, Park A, Busch M, Bird J, Zheng X, et al. Site-specific antibody-drug conjugation through glycoengineering. Bioconjugate Chem. 2014;25(3):510–20. doi:10.1021/bc400505q.
11. O'Shannessy DJ, Dobersen MJ, Quarles RH. A novel procedure for labeling immunoglobulins by conjugation to oligosaccharide moieties. Immunol Lett. 1984;8(5):273–77. doi:10.1016/0165-2478(84)90008-7.
12. Ramakrishnan B, Qasba PK. Structure-based design of β1,4-galactosyltransferase I (β4Gal-T1) with equally efficient *N*-acetylgalactosaminyltransferase activity: point mutation broadens β4Gal-T1 donor specificity. J Biol Chem. 2002;277(23):20833–39. doi:10.1074/jbc.M111183200.
13. Thompson P, Ezeadi E, Hutchinson I, Fleming R, Bezabeh B, Lin J, Mao S, Chen C, Masterson L, Zhong H, et al. Straightforward glycoengineering approach to site-specific antibody-pyrrolobenzodiazepine conjugates. ACS Med Chem Lett. 2016;7(11):1005–08. doi:10.1021/acsmedchemlett.6b00278.
14. Zhu Z, Ramakrishnan B, Li J, Wang Y, Feng Y, Prabakaran P, Colantonio S, Dyba MA, Qasba PK, Dimitrov DS. Site-specific antibody-drug conjugation through an engineered glycotransferase and a chemically reactive sugar. MAbs. 2014;6:1190–200. doi:10.4161/mabs.29889.
15. Li X, Fang T, Boons GJ. Preparation of well-defined antibody-drug conjugates through glycan remodeling and strain-promoted azide-alkyne cycloadditions. Angew Chem Int Ed Engl. 2014;53:7179–82. doi:10.1002/anie.201402606.
16. van Geel R, Wijdeven MA, Heesbeen R, Verkade JM, Wasiel AA, van Berkel SS, van Delft FL. Chemoenzymatic conjugation of toxic payloads to the globally conserved *N*-glycan of native mAbs provides homogeneous and highly efficacious antibody-drug conjugates. Bioconjugate Chem. 2015;26(11):2233–42. doi:10.1021/acs.bioconjchem.5b00224.
17. Wijdeven MA, van Geel R, Hoogenboom JH, Verkade JMM, Janssen BMG, Hurkmans I, de Bever L, van Berkel SS, van Delft FL. Enzymatic glycan remodeling-metal free click (GlycoConnect^{TM}) provides homogenous antibody-drug conjugates with improved stability and therapeutic index without sequence engineering. MAbs. 2022;14(1):2078466. doi:10.1080/19420862.2022.2078466.
18. Deslignière E, Ehkirch A, Duivelshof BL, Toftevall H, Sjogren J, Guillarme D, D'Atri V, Beck A, Hernandez-Alba O, Cianferani S. State-of-the-art native mass spectrometry and ion mobility methods to monitor homogeneous site-specific antibody-drug conjugates synthesis. Pharm. 2021:14. doi:10.3390/ph14060498.
19. Adumeau P, Raave R, Boswinkel M, Heskamp S, Wessels H, van Gool AJ, Moreau M, Bernhard C, Da Costa L, Goncalves V, et al. Site-specific, platform-based conjugation strategy for the synthesis

of dual-labeled immunoconjugates for bimodal PET/NIRF imaging of HER2-positive tumors. Bioconjugate Chem. 2022;33:530–40. doi:10.1021/acs.bioconjchem.2c00049.
20. Verkade JMM, Wijdeven MA, Van Geel R, Janssen BMG, Van Berkel SS, Van Delft FL. A polar sulfamide spacer significantly enhances the manufacturability, stability, and therapeutic index of antibody-drug conjugates. Antibodies. 2018:7. doi:10.3390/antib7010012.
21. Tang F, Wang LX, Huang W. Chemoenzymatic synthesis of glycoengineered IgG antibodies and glycosite-specific antibody-drug conjugates. Nat Protoc. 2017;12(8):1702–21. doi:10.1038/nprot.2017.058.
22. Zhang X, Ou C, Liu H, Prabhu SK, Li C, Yang Q, Wang LX. General and robust chemoenzymatic method for glycan-mediated site-specific labeling and conjugation of antibodies: facile synthesis of homogeneous antibody-drug conjugates. ACS Chem Biol. 2021;16(11):2502–14. doi:10.1021/acschembio.1c00597.
23. Shi W, Li W, Zhang J, Li T, Song Y, Zeng Y, Dong Q, Lin Z, Gong L, Fan S, et al. One-step synthesis of site-specific antibody-drug conjugates by reprograming IgG glycoengineering with LacNAc-based substrates. Acta Pharm Sin B. 2022;12(5):2417–28. doi:10.1016/j.apsb.2021.12.013.
24. Zhang X, Ou C, Liu H, Wang LX. Synthesis and evaluation of three azide-modified disaccharide oxazolines as enzyme substrates for single-step Fc Glycan-mediated antibody-drug conjugation. Bioconjugate Chem. 2022;33(6):1179–91. doi:10.1021/acs.bioconjchem.2c00142.
25. Xu X, Nagarajan H, Lewis NE, Pan S, Cai Z, Liu X, Chen W, Xie M, Wang W, Hammond S, et al. The genomic sequence of the Chinese hamster ovary (CHO)-K1 cell line. Nat Biotechnol. 2011;29(8):735–41. doi:10.1038/nbt.1932.
26. Arnold JN, Wormald MR, Sim RB, Rudd PM, Dwek RA. The impact of glycosylation on the biological function and structure of human immunoglobulins. Annu Rev Immunol. 2007;25:21–50. doi:10.1146/annurev.immunol.25.022106.141702.
27. Jefferis R. Glycosylation of recombinant antibody therapeutics. Biotechnol Prog. 2005;21(1):11–16. doi:10.1021/bp040016j.
28. van de Bovenkamp FS, Hafkenscheid L, Rispens T, Rombouts Y. The emerging importance of IgG Fab Glycosylation in immunity. J Immunol. 2016;196(4):1435–41. doi:10.4049/jimmunol.1502136.
29. Qian J, Liu T, Yang L, Daus A, Crowley R, Zhou Q. Structural characterization of N-linked oligosaccharides on monoclonal antibody cetuximab by the combination of orthogonal matrix-assisted laser desorption/ionization hybrid quadrupole-quadrupole time-of-flight tandem mass spectrometry and sequential enzymatic digestion. Anal Biochem. 2007;364(1):8–18. doi:10.1016/j.ab.2007.01.023.
30. Qu Z, Sharkey RM, Hansen HJ, Shih LB, Govindan SV, Shen J, Goldenberg DM, Leung SO. Carbohydrates engineered at antibody constant domains can be used for site-specific conjugation of drugs and chelates. J Immunol Methods. 1998;213(2):131–44. doi:10.1016/s0022-1759(97)00192-0.
31. Janin-Bussat MC, Tonini L, Huillet C, Colas O, Klinguer-Hamour C, Corvaia N, Beck A. Cetuximab Fab and Fc *N*-glycan fast characterization using IdeS digestion and liquid chromatography coupled to electrospray ionization mass spectrometry. Methods Mol Biol. 2013;988:93–113. doi:10.1007/978-1-62703-327-5_7.
32. Bosques CJ, Collins BE, Meador JW 3rd, Sarvaiya H, Murphy JL, Dellorusso G, Bulik DA, Hsu IH, Washburn N, Sipsey SF, et al. Chinese hamster ovary cells can produce galactose-α-1,3-galactose antigens on proteins. Nat Biotechnol. 2010;28(11):1153–56. doi:10.1038/nbt1110-1153.
33. Donini R, Haslam SM, Kontoravdi C. Glycoengineering Chinese hamster ovary cells: a short history. Biochem Soc Trans. 2021;49(2):915–31. doi:10.1042/BST20200840.
34. Giddens JP, Lomino JV, DiLillo DJ, Ravetch JV, Wang LX. Site-selective chemoenzymatic glycoengineering of Fab and Fc glycans of a therapeutic antibody. Proc Natl Acad Sci U S A. 2018;115(47):12023–27. doi:10.1073/pnas.1812833115.
35. Wakarchuk WW, Cunningham AM. Capillary electrophoresis as an assay method for monitoring glycosyltransferase activity. Methods Mol Biol. 2003;213:263–74. doi:10.1385/1-59259-294-5:263.
36. Watson DC, Wakarchuk WW, Gervais C, Durocher Y, Robotham A, Fernandes SM, Schnaar RL, Young NM, Gilbert M. Preparation of legionaminic acid analogs of sialo-glycoconjugates by means of mammalian sialyltransferases. Glycoconjugate J. 2015;32(9):729–34. doi:10.1007/s10719-015-9624-4.
37. Stuible M, Burlacu A, Perret S, Brochu D, Paul-Roc B, Baardsnes J, Loignon M, Grazzini E, Durocher Y. Optimization of a high-cell-density polyethylenimine transfection method for rapid protein production in CHO-EBNA1 cells. J Biotechnol. 2018;281:39–47. doi:10.1016/j.jbiotec.2018.06.307.
38. Hornak V, Abel R, Okur A, Strockbine B, Roitberg A, Simmerling C. Comparison of multiple Amber force fields and development of improved protein backbone parameters. Proteins. 2006;65(3):712–25. doi:10.1002/prot.21123.
39. Kirschner KN, Yongye AB, Tschampel SM, Gonzalez-Outeirino J, Daniels CR, Foley BL, Woods RJ. GLYCAM06: a generalizable biomolecular force field. Carbohydr J Comput Chem. 2008;29(4):622–55. doi:10.1002/jcc.20820.
40. Gupta R, Brunak S. Prediction of glycosylation across the human proteome and the correlation to protein function. Pac Symp Biocomput. 2002;7:310–22.
41. Raymond C, Robotham A, Spearman M, Butler M, Kelly J, Durocher Y. Production of α2,6-sialylated IgG1 in CHO cells. MAbs. 2015;7(3):571–83. doi:10.1080/19420862.2015.1029215.
42. Huang HS, Nagane M, Klingbeil CK, Lin H, Nishikawa R, Ji XD, Huang CM, Gill GN, Wiley HS, Cavenee WK. The enhanced tumorigenic activity of a mutant epidermal growth factor receptor common in human cancers is mediated by threshold levels of constitutive tyrosine phosphorylation and unattenuated signaling. J Biol Chem. 1997;272(5):2927–35. doi:10.1074/jbc.272.5.2927.